

# Effect of Three-body Interaction on Phase Transition of Hot Asymmetric Nuclear Matter

W. Zuo<sup>1,2,3\*</sup>, Z.H. Li<sup>1,2</sup>, A.Li<sup>3</sup>, U. Lombardo<sup>4</sup>

<sup>1</sup> *Institute of Modern Physics, Chinese Academy of Sciences, Lanzhou 730000, P.R. China*

<sup>2</sup> *Graduate School of Chinese Academy of Sciences, Beijing 100039, P. R. China*

<sup>3</sup> *School of Physics and Technology,  
Lanzhou University, Lanzhou 730000, P. R. China*

<sup>4</sup> *INFN-LNS, Via Santa Sofia 44, I-95123 Catania, Italy*

The properties and the isospin dependence of the liquid-gas phase transition in hot asymmetric nuclear matter have been investigated within the framework of the finite temperature Brueckner-Hartree-Fock approach extended to include the contribution of a microscopic three-body force. A typical Van der Waals structure has been observed in the calculated isotherms (of pressure) for symmetric nuclear matter implying the presence of the liquid-gas phase transition. The critical temperature of the phase transition is calculated and its dependence on the proton-to-neutron ratio is discussed. It is shown that the three-body force gives a repulsive contribution to the nuclear equation of state and reduces appreciably the critical temperature and the mechanical instable region. At fixed temperature and density the pressure of asymmetric nuclear matter increases monotonically as a function of isospin asymmetry. In addition, it turns out that the domain of mechanical instability for hot asymmetric nuclear matter gradually shrinks with increasing asymmetry and temperature. We have compared our results with the predictions of other theoretical models especially the Dirac Brueckner approach. A possible explanation for the discrepancy between the values of the critical temperature predicted by the present non-relativistic Brueckner calculations including the three-body force and the relativistic Dirac-Brueckner method is given.

**PACS numbers:** 21.65.+f, 13.75.Cs, 24.10.Cn, 05.70.Fh

---

\* Corresponding address: Institute of Modern Physics, Chinese Academy of Science, P.O.Box 31, Lanzhou 730000, China. Tel: 0086-931-4969318; E-mail: zuowei@impcas.ac.cn

## I. INTRODUCTION

The determination of the properties of nuclear matter as a function of temperature, density and isospin asymmetry is one of the fundamental subjects in nuclear physics. For a long time it has been expected that, due to the Van der Waals nature of the nucleon-nucleon (NN) interaction, nuclear matter is likely to exhibit a liquid-gas phase transition at low densities and moderate temperatures[1]. Phase transition is a phenomenon of great and extensive interests observed or expected in various fields, such as melting or boiling in condensed matters and atomic clusters[2, 3], decay of hot nuclei[4, 5] and transition to quark-gluon plasma in high energy heavy ion collisions and neutron stars[6]. In heavy ion collisions at intermediate and high energies, hot asymmetric nuclear matter can be produced and during the expansion stage of the collisions the liquid-gas phase transition may occur depending on the temperatures and densities involved[7, 8]. Besides its general interest in nuclear physics, the equation of state (EOS) of hot asymmetric nuclear matter plays also an essential role in understanding many astrophysical phenomena related to the dynamics of supernova explosions and the evolution of the protoneutron star formed in the latest stage of a type-II supernova collapse[9]. It is therefore highly desirable to predict on a microscopic basis the thermal properties of asymmetric nuclear matter at finite temperature which provide a starting point for the physics of heavy ions[10, 11] and protoneutron stars[12].

Within various theoretical models such as the phenomenological non-relativistic Skyrme force models[13, 14] and the relativistic mean field theory (RMT)[8], the EOS of hot nuclear matter has been studied extensively. All of these investigations have predicted a Van der Waals behavior for infinite symmetric nuclear matter. The critical temperature  $T_c$  of the liquid-gas phase transition turns out to be in the range from 14 MeV to 20 MeV depending on the adopted models and NN interactions. Based on realistic NN interactions, the EOS of cold nuclear matter has been explored by many physicists within the variational method[15], the non-relativistic Brueckner-Hartree-Fock (BHF) approach[16, 17] and the Dirac Brueckner (DB) theory[18, 19]. However, the investigations of hot asymmetric nuclear matter from the microscopic models are relatively rare. In Ref.[20], the liquid-gas phase transition has been

predicted for symmetric nuclear matter by using the variational method based on the Argonne  $V_{14}$  two-body NN interaction plus a phenomenological three-body force and the critical temperature obtained is about 17.5 MeV close to the values from the Skyrme force calculations. On the contrary, it is reported in Ref.[21] from the finite temperature DB calculations an almost complete destruction of Van der Waals like behavior. As been discussed in Ref.[22], this unusual result in the DB framework has not been well understood and deserves deeper investigations. In a more recent work[23], the Van der Waals structure has been obtained in the DB framework, but the predicted critical temperature is as low as  $\sim 10\text{MeV}$ . In Ref.[24], the properties of hot asymmetric nuclear matter has been studied in the finite temperature BHF approach by adopting the separable version of the Paris two-body force. As well known, within a non-relativistic microscopic framework three-body forces are decisive for reproducing the empirical saturation properties of cold nuclear matter and in the zero-temperature case their contribution shifts the EOS close to the one of the relativistic DB calculations[25]. In the present paper, our aim is to explore the EOS of hot asymmetric nuclear matter in the finite temperature BHF approach extended to include the contribution of the microscopic three-body force (TBF) constructed from the meson exchange current model[26]. We shall stress the isospin dependence of the liquid-gas phase transition and the effect of the TBF in particular its possible connection to the relativistic effect in the DB approach. In the present calculations, the Argonne  $V_{18}$  ( $AV_{18}$ ) potential[27] has been adopted as the realistic two-body interaction. The paper is arranged as follows. In the next section we give a brief description of the theoretical approaches. The numerical results are presented and discussed in Section III. Finally a summary is given in Sect.IV.

## II. THEORETICAL MODELS

### A. Temperature-dependent Effective Three-body Force

The microscopic TBF adopted in the present calculations is constructed from the meson-exchange current approach [26] and its components are displayed dia-

grammatically in Fig.1, taken from Ref.[26]. Four important mesons  $\pi$ ,  $\rho$ ,  $\sigma$  and  $\omega$  are considered[28]. The TBF model contains the contribution of the two-meson exchange part of the NN interaction medium-modified by the intermediate virtual excitation of nucleon resonances, the term associated to the non-linear meson-nucleon coupling required by the chiral symmetry, the simplest contribution rising from meson-meson interaction and finally, the two-meson exchange diagram with the virtual excitations of nucleon-antinucleon pairs. The meson masses in the TBF have been fixed at their physical values except for the virtual  $\sigma$ -meson mass which has been fixed at 540MeV according to Ref. [26]. This value has been checked to satisfactorily reproduce the  $AV_{18}$  interaction from the one-boson-exchange potential (OBEP) model[25]. The other parameters of the TBF, i.e., the coupling constants and the form factors, have been determined from the OBEP model to meet the self-consistent requirement with the adopted  $AV_{18}$  two-body force. The parameters of the TBF is given in Ref.[25]. A more detailed description of the model and the approximations can be found in Refs. [25, 26].

In the zero-temperature case, the TBF contribution has been included in the BHF calculations by constructing an effective two-body interaction via a suitable average with respect to the third-nucleon degrees of freedom[26, 29]. By extending the standard scheme adopted for the zero-temperature case, one can reduce the TBF to a temperature dependent effective two-body force  $V_3^{\text{eff}}(T)$  which reads in  $r$ -space,

$$\begin{aligned} \langle \vec{r}_1' \vec{r}_2' | V_3^{\text{eff}}(T) | \vec{r}_1 \vec{r}_2 \rangle &= \frac{1}{4} \text{Tr} \sum_{k_n} f(k_n, \rho, \beta, T) \int d\vec{r}_3 d\vec{r}_3' \phi_n^*(\vec{r}_3') (1 - \eta(r_{13}', T)) \\ &\times (1 - \eta(r_{23}', T)) W_3(\vec{r}_1' \vec{r}_2' \vec{r}_3' | \vec{r}_1 \vec{r}_2 \vec{r}_3) \\ &\times \phi_n(r_3) (1 - \eta(r_{13}, T)) (1 - \eta(r_{23}, T)), \end{aligned} \quad (1)$$

where the trace is taken with respect to spin and isospin of the third nucleon. The function  $\eta(r, T)$  is the defect function[26, 29, 31] which is defined as  $\eta(r, T) = \phi(r) - \psi(r, T)$ , where  $\psi(r, T)$  is the correlated wave function for the relative motion of two nucleons in nuclear medium and  $\phi(r)$  is the corresponding unperturbed one. A detailed description and justification of the above scheme can be found in Ref.[26].

It is worth stressing that the TBF itself, i.e.  $W_3$ , is the same as the one adopted in our previous calculations for the zero-temperature case[25] and it is independent

of temperature. However, in the finite-temperature case, the effective two-body force  $V_3^{\text{eff}}(T)$  constructed from the TBF depends on temperature in an implicitly complicated way due to the medium effects. As a consequence the contribution of the TBF is expected to be more pronounced at finite temperature. It is clear from Eq.(1) that the temperature dependence of  $V_3^{\text{eff}}(T)$  stems from the Fermi distribution  $f(k, \rho, \beta, T)$  and the defect function  $\eta(r, T)$  which is strongly temperature dependent. We will return to this point in the next subsection.

## B. Finite Temperature Brueckner-Hartree-Fock Approach

In general, three independent parameters are required to specify a given thermodynamical state of hot asymmetric nuclear matter, i.e., the total nucleon number density  $\rho$ , the isospin asymmetry parameter  $\beta = (\rho_n - \rho_p)/\rho$  and the temperature  $T$ . At zero temperature, the neutron and proton Fermi momenta are related to their respective number densities  $\rho_n = (1 + \beta)\rho/2$  and  $\rho_p = (1 - \beta)\rho/2$  by  $k_F^\tau = [3\pi^2\rho_\tau]^{1/3}$  with  $\tau = p$  or  $\tau = n$ . The Brueckner-Bethe-Goldstone (BBG) approach for cold asymmetric nuclear matter is described in Ref.[16, 17]. The extension to finite temperature is given in Ref.[24]. In the following, we give a brief review for completeness. The starting point of the BBG approach is the Brueckner reaction  $G$  matrix which satisfies the following generalized Bethe-Goldstone (BG) equation[16],

$$G_{\tau,\tau'}(\rho, \beta, T, \omega) = v + v \sum_{k_1 k_2} \frac{|k_1 k_2\rangle Q_{\tau,\tau'}(k_1, k_2) \langle k_1 k_2|}{\omega - \epsilon_\tau(k_1) - \epsilon_{\tau'}(k_2)} G_{\tau,\tau'}(\rho, \beta, T, \omega), \quad (2)$$

where  $v = v_2 + V_3^{\text{eff}}(T)$  is the NN interaction and  $\omega$  is the starting energy. In the present calculations the  $AV_{18}$  potential is adopted as the bare two-body force  $v_2$  and the TBF contribution is included via the effective interaction  $V_3^{\text{eff}}(T)$  given by Eq.(1). Since the defect function is determined by the  $G$  matrix, the effective force  $V_3^{\text{eff}}$  should be evaluated self-consistently with the BG equation at each step of the Brueckner iteration. In Eq.(2), the single particle (s.p.) energy is defined as  $\epsilon_\tau(k) \equiv \epsilon_\tau(k, \rho, \beta, T) = \hbar^2 k^2/(2m) + U_\tau(k, \rho, \beta, T)$ . In the present calculations, we adopt the continuous choice[30] for the s.p. potential  $U_\tau(k) \equiv U_\tau(k, \rho, \beta, T)$  since it is a natural choice for  $T \neq 0$ [31, 32] and it provides a much faster convergence of the hole-line expansion in the zero-temperature limit than the gap choice[33]. The

s.p. potential is calculated from the real part of on-shell  $G$  matrix,

$$U_\tau(k, \rho, \beta, T) = \frac{1}{2} \sum_{\tau'} \sum_{\vec{k}'} f_{\tau'}(k', \rho, \beta, T) \langle kk' | G_{\tau, \tau'}(\rho, \beta, T, \epsilon_\tau(k) + \epsilon_{\tau'}(k')) | kk' \rangle_A, \quad (3)$$

where the subscript  $A$  denotes the anti-symmetrization of the matrix elements. The finite temperature Pauli operator is simply an extension of the zero-temperature one, i.e.,

$$Q_{\tau, \tau'}(k_1, k_2) \equiv Q_{\tau, \tau'}(k_1, k_2, \rho, \beta, T) = [1 - f_\tau(k_1, \rho, \beta, T)][1 - f_{\tau'}(k_2, \rho, \beta, T)]. \quad (4)$$

In Eq.(2), the Pauli operator is applied only for the intermediate states of momenta  $k_1, k_2$ . The Fermi distribution for  $T \neq 0$  is expressed as,

$$f_\tau(k, \rho, \beta, T) = \left[ 1 + \exp \left( \frac{\epsilon_\tau(k) - \mu_\tau}{T} \right) \right]^{-1}, \quad (5)$$

where  $\mu_\tau = \mu_\tau(k, \rho, T)$  is the chemical potential. For any given density and temperature, we can calculate the chemical potential  $\mu_\tau$  from the following implicit equation self-consistently by iteration,

$$\rho_\tau = \frac{1}{V} \sum_k f_\tau(k, \rho, \beta, T) = \frac{1}{V} \sum_k \left[ 1 + \exp \left( \frac{\epsilon_\tau(k) - \mu_\tau}{T} \right) \right]^{-1}. \quad (6)$$

The BG equation can be expended in partial waves as in the zero-temperature case[31]. The resulting equations in different partial waves are coupled with each other due to the angular dependence of the Pauli operator and the s.p. energy. To remove the angular dependence, we approximate the exact Pauli operator and s.p. energy in the BG equation by their angle-averaged values. For instance, the angle average of the Pauli operator is expressed as,

$$\langle Q_{\tau\tau'}(q, P, \rho, \beta, T) \rangle = \frac{1}{2} \int_0^\pi \sin \theta d\theta [1 - f_\tau(k_1, \rho, \beta, T)][1 - f_{\tau'}(k_2, \rho, \beta, T)], \quad (7)$$

where  $\vec{q} = (\vec{k}_1 - \vec{k}_2)/2$  and  $\vec{P} = \vec{k}_1 + \vec{k}_2$  are the relative momentum and the total momentum of the two nucleons, respectively.  $\theta$  is the angle between  $\vec{q}$  and  $\vec{P}$ . In the case of  $T = 0$ , the angle-average of the Pauli operator can be derived analytically due to the sharp Fermi distribution at  $T = 0$ [16, 17, 18]. Whereas for  $T \neq 0$ , the integral in Eq.(7) can not be worked out explicitly and one has to evaluate the angle-average of the Pauli operator numerically. In the present paper, the integral in

Eq.(7) is calculated numerically by the Gauss-Legendre method. We have checked that in the zero-temperature limit our numerical results can reproduce the analytical values with very high accuracy.

The energy per nucleon of asymmetric nuclear matter at the BHF level of approximation is given by,

$$E(\rho, \beta, T) = \sum_{\tau} \sum_k f_{\tau}(k, \rho, \beta, T) \frac{\hbar^2 k^2}{2m} + \frac{1}{2} \sum_{\tau, \tau'} \sum_{k, k'} f_{\tau}(k, \rho, \beta, T) f_{\tau'}(k', \rho, \beta, T) \times \langle kk' | G_{\tau, \tau'}(\rho, \beta, T, \epsilon(k) + \epsilon(k')) | kk' \rangle_A. \quad (8)$$

At the mean field approximation, the total entropy  $S$  is expressed as[24]

$$S = - \sum_{\tau} \sum_k \{ f_{\tau}(k, \rho, \beta, T) \ln f_{\tau}(k, \rho, \beta, T) + [1 - f_{\tau}(k, \rho, \beta, T)] \ln [1 - f_{\tau}(k, \rho, \beta, T)] \} \quad (9)$$

The free energy  $F$  is calculated according to the standard thermodynamic relation  $F = E - TS$  and the pressure  $P$  is then extracted from the free energy by performing a numerical derivative, i.e.,

$$P = \rho^2 \left( \frac{\partial F}{\partial \rho} \right)_{T, \beta}. \quad (10)$$

According to Ref.[8] the criteria for mechanical stability can be straightforwardly expressed as follows

$$\rho^2 \left( \frac{\partial^2 F}{\partial \rho^2} \right)_{T, \beta} = \rho \left( \frac{\partial P}{\partial \rho} \right)_{T, \beta} > 0.$$

The set of coupled equations (2), (3) and (6) is referred to as the finite temperature BHF approximation (FTBHF)[24]. When the TBF contribution is included, this set of equations has to be solved self-consistently along with Eq.(1) to get the  $G$  matrix. Hereafter we will call the FTBHF including the TBF contribution as the extended FTBHF.

As a check of the extended model, we have calculated the speed of sound in cold symmetric nuclear matter, i.e.,  $s/c = \left( \frac{dP}{d\varepsilon} \right)^{1/2}$ , where  $c$  represents the speed of light and  $\varepsilon$  refers to the total energy density. The results are shown in Tab. 1 for several densities. In the table the result including the TBF contribution is denoted by BHF( $AV_{18}$  + TBF), while the one without the TBF by BHF( $AV_{18}$ ). It is seen that in both cases with and without the TBF, the calculated speed of sound fulfills the causality condition  $s/c < 1$  in the relevant density region. Below a certain value of

density ( $\sim 0.14\text{fm}^{-3}$  in the case without the TBF and  $\sim 0.11\text{ fm}^{-3}$  with the TBF) the speed of sound  $s/c$  becomes imaginary due to the mechanical instability.

TABLE I: Speed of sound  $s/c$  in symmetric nuclear matter for several values of density in both cases, with and without the TBF.

$\rho(\text{fm}^{-3})$	0.15	0.20	0.25	0.30	0.35	0.40	0.45
BHF( $AV_{18}$ )	0.01	0.08	0.15	0.20	0.25	0.29	0.35
BHF( $AV_{18} + \text{TBF}$ )	0.07	0.16	0.24	0.33	0.42	0.51	0.59

### III. NUMERICAL RESULTS AND DISCUSSIONS

The EOS of asymmetric nuclear matter is reported in Fig.2 for four values of asymmetry parameter  $\beta = 0, 0.3, 0.5, 0.8$ , where the solid and dashed isothermal curves of pressure (corresponding to  $T = 0, 8, 10, 12, 14, 16\text{MeV}$  from the bottom to the top) indicate the results with and without the TBF contribution, respectively. From the figure one can see that for both cases with and without the TBF, the EOS of symmetric nuclear matter ( $\beta = 0$ ) displays a typical Van der Waals behavior, implying that the infinite nuclear system may undergo a liquid-gas phase transition. The critical temperature and density of the phase transition is determined by the condition  $\left(\frac{\partial P}{\partial \rho}\right)_{T,\beta} = \left(\frac{\partial^2 P}{\partial \rho^2}\right)_{T,\beta} = 0$ . From the calculated isotherms of pressure, one can extract the critical temperature  $T_c$  and the critical density  $\rho_c$ . In the case without the TBF contribution, the obtained  $T_c$  is approximately 16 MeV which is in the range of 15–20 MeV predicted by the Skyrme-Hartree-Fock (SHF) calculations[13]. As expected, the TBF gives a repulsive contribution to the nuclear EOS. In the zero-temperature case, the additional repulsion from the TBF improves greatly the predicted saturation density of cold symmetric nuclear matter. The equilibrium properties of cold nuclear matter have been reported in Ref.[25]. At higher temperature, the TBF effect becomes more pronounced due to the temperature dependence of its contribution (i.e., the effective force  $V_3^{\text{eff}}(T)$ ). Inclusion of the TBF contribution reduces the critical temperature from  $\sim 16$  MeV to  $\sim 13$  MeV which is close



to the value of  $\sim 14$  MeV from the relativistic mean field theory[8]. The reduction of  $T_c$  due to the TBF may be attributed largely to the medium and temperature dependence of the reduced effective interaction  $V_3^{\text{eff}}(T)$ , i.e., at a fixed temperature the TBF contribution is stronger for larger density and for a given density it is more pronounced at higher temperature. The calculated critical density  $\rho_c$  of the phase transition is roughly  $0.065 \text{ fm}^{-3}$  and  $0.08 \text{ fm}^{-3}$  in the two cases with and without the TBF, respectively. Both values are in the density range of  $\rho_0/3 \sim \rho_0/2$  in agreement with other investigations[8, 13, 14, 23]. The TBF reduces the critical density since its contribution to the nuclear EOS is repulsive and increases as a function of density.

Now let us compare our result with the predictions of other approaches. In Ref.[20], the liquid-gas phase transition of hot nuclear matter has been studied with the variational method by adopting the Argonne  $V_{14}$  two-body NN interaction supplemented with a phenomenological TBF. The obtained value of  $T_c$  in Ref.[20] is about 17.5 MeV which is higher than the present value  $T_c \sim 13\text{MeV}$  from the BHF approach when the TBF contribution is included. This disagreement concerning the critical temperature might be attributed to the two different approaches and to the different NN interactions adopted. As it has been noticed in Ref.[36], the density dependence of the symmetry energy predicted from the two methods differs remarkably from each other even when the same NN interaction has been used. The reason for the discrepancy between the results of the two methods remains largely unclear as discussed in Ref.[17].

In the relativistic DB framework, the EOS of hot nuclear matter has been investigated in Refs.[21, 23] where the extension to finite temperature has been achieved by the inclusion of the finite temperature Green's functions[34]. Such an extension coincides in the non-relativistic limit with the one adopted in the present FTBHF calculations. In Ref.[21], the reported EOS does not display any Van der Waals like behavior in contrast to the results obtained from other approaches such as the non-relativistic BHF, the SHF, the variational method, and the RMT. As discussed in Ref.[22] this discrepancy is not easy to be understood since the inclusion of the TBF in the BHF calculations is expected to give a similar behavior of the EOS to that of the DB approach. One possible reason for that is that in the calculations of

Ref.[21], the  $\Delta$ -resonance has been included explicitly which produces an additional repulsion to the EOS and makes nuclear matter less bound. In a later work[23], the problem has been re-visited in the DB approach and a clear Van der Waals structure is observed in the calculated EOS. However, the obtained critical temperature  $T_c \simeq 10$  MeV in Ref.[23] is considerably lower than the value of  $\sim 13$  MeV in the present work. As pointed out in Refs.[22, 35] that the main relativistic effect in the DB approach is associated to the contribution (of the TBF) due to the  $2\sigma$ -exchange process coupled to the virtual excitation of a nucleon-antinucleon pair which is referred to as  $2\sigma-N\bar{N}$  TBF in Refs.[25, 26]. In our previous investigations[25], it is shown that the most important relativistic correction to the nuclear EOS can be fairly well reproduced by the BHF calculation including only the  $2\sigma-N\bar{N}$  contribution of the TBF. This implies that the full TBF in the present calculations is not completely equivalent to the relativistic effect in DB approach especially in the finite-temperature case for which both the relativistic and the TBF effects are expected to become more pronounced as compared to the zero-temperature case. In order to get a deeper insight into the disagreement of the predicted critical temperature between the DB approach and the FTBHF approach with the TBF contribution, we separate the  $2\sigma-N\bar{N}$  contribution from the full TBF. The results are given in Fig.3 where the solid curves are obtained by including only the  $2\sigma-N\bar{N}$  contribution and the dashed curves by adopting the full TBF. It is seen that the contribution of the full TBF is somewhat less repulsive than that of the  $2\sigma-N\bar{N}$  component. As a consequence, the value of  $T_c$  is lowered from  $\sim 13$  MeV to  $\sim 11$  MeV if only the  $2\sigma-N\bar{N}$  contribution in the TBF is taken into account. This result is compatible with our previous one for the zero-temperature case[25] and provides a possible explanation for the above mentioned discrepancy.

As well known, pure neutron matter is unbound, therefore it is interesting to discuss the isospin dependence of the phase transition. By comparing the results for different isospin asymmetries (Fig.2a,b,c and d), one can see that as the isospin asymmetry increases, the Van der Waals structure of the EOS becomes less pronounced and the mechanical instable region where the pressure decreases as a function of density, gets smaller. This indicates that the critical temperature drops down monotonically as the asymmetry increases in both cases with and without the TBF,

in agreement with the results obtained from the isospin lattice gas model[37]. The TBF gives a repulsive contribution to the EOS. The repulsion of the TBF becomes stronger as the density increases and consequently reduces the critical temperature in the whole range of asymmetry. When the asymmetry is high enough, the region of mechanical instability vanishes for all values of temperature. The extracted critical asymmetry  $\beta_c$  for the disappearance of the mechanical instability is about 0.85 in the case without the TBF contribution. Inclusion of the TBF reduces  $\beta_c$  to about 0.75. It is also seen that at a fixed asymmetry, the mechanical unstable domain of the system gets smaller as the temperature becomes higher.

In Fig.4 is shown the pressure as a function of density at a fixed temperature  $T = 5$  MeV for different values of asymmetry  $\beta = 0.0, 0.2, 0.4, 0.6, 0.8, 1.0$ . In the figure, the solid curves and dashed curves correspond to the results with and without the TBF contribution. It can be observed from the figure that the pressure increases monotonically as the isospin asymmetry increases in agreement with the results of the RMT calculations[8] where it is shown that for asymmetric nuclear matter ( $\beta \neq 0$ ) which is a two-component system, the pressure cannot remain a constant during the liquid-gas phase transition. In the cases of  $\beta = 0.0, 0.2, 0.4, 0.6$ , the system exhibit a mechanical instability where the pressure is a decreasing function of density. However for high enough asymmetry, especially for pure neutron matter ( $\beta = 1$ ), the pressure becomes an monotonically increasing function of density, which indicates the disappearing of the mechanical instability at all densities. The TBF gives a repulsive contribution in the whole asymmetry range  $0 \leq \beta \leq 1$ .

In order to illustrate more clearly the TBF effect on the properties of the phase transition in asymmetric nuclear matter, we plot in Fig.5 the domain of mechanical instability in density-asymmetry plane for the fixed temperature  $T = 5$  MeV. In the figure, the solid and dashed curves are obtained by adopting the  $AV_{18}$  plus the TBF and the pure  $AV_{18}$  two-body force, respectively. From the figure we can see that inclusion of the TBF contribution suppresses considerably the region of mechanical instability in isothermal asymmetric nuclear matter. In addition, the TBF effect on the lower-density boundary of the mechanical instable region is very small but it leads to a remarkable reduction of the upper-density boundary. This is expected since the TBF repulsion becomes stronger at higher densities.

#### IV. SUMMARY

In the present work, we have introduced the microscopic TBF into the framework of the finite temperature BHF approach. Employing the extended theoretical model, we have investigated the EOS and the properties of the liquid-gas phase transition for hot asymmetric nuclear matter. For symmetric nuclear matter, the calculated EOS exhibits a clear Van der Waals behavior in the pressure-density plane, which implies the presence of a liquid-gas phase transition. The extracted critical temperature is about 16 MeV in the case without the TBF contribution. It is shown that the TBF gives a repulsive contribution to the EOS and its effect becomes stronger as increasing density. When the TBF contribution is included, the critical temperature turns out to be reduced by about 3 MeV from  $T_c \approx 16$  MeV to  $T_c \approx 13$  MeV as compared to the corresponding two-body force predictions. The predicted value of  $T_c \approx 13$  MeV is close to the value  $T_c \simeq 14$  MeV obtained from the RMT[8] but it is appreciably larger than that of the relativistic DB approach. If including only the  $2\sigma - N\bar{N}$  contribution of the TBF, we obtain a lower value of  $T_c \approx 11$  MeV which is close to the value of about 10 MeV predicted by the DB calculations in Ref.[23]. This result is desirable since it may provide a possible explanation for the discrepancy between the critical temperature values obtained from the DB approach and the present BHF plus TBF calculations, i.e, except the  $2\sigma - N\bar{N}$  contribution, the other components of the TBF do not completely cancel among each others at least for the case of finite temperature and their net effect may becomes more pronounced at higher temperature. The critical density  $\rho_c$  is found to be roughly  $0.065 \text{ fm}^{-3}$  and  $0.08 \text{ fm}^{-3}$  in the cases with and without the TBF contribution, respectively. Both values are in the range between  $\rho_0/3$  and  $\rho_0/2$ .

For asymmetric nuclear matter, the isospin dependence of the properties of the liquid-gas phase transition has been studied. It turns out that the critical temperature decreases and the mechanical instable region gradually shrinks as the isospin asymmetry  $\beta$  increases in both cases with and without the TBF. The contribution of the TBF to the EOS is repulsive in the whole range of asymmetry  $0 \leq \beta \leq 1$  and results in a reduction of the critical temperature for the phase transition in hot asymmetric nuclear matter. Above a critical value of asymmetry, the mechanical

instability disappears for all values of temperature. The addition repulsion due to the TBF lowers the critical asymmetry for the disappearance of the mechanical instability and makes the asymmetric nuclear matter easier to be gasified. At fixed temperature and density the pressure in hot asymmetric nuclear system turns out to be a monotonically increasing function of asymmetry parameter. In addition, it is also shown that at a fixed asymmetry the mechanical unstable region of hot asymmetric nuclear matter shrinks as increasing temperature.

## V. ACKNOWLEDGMENT

One of us (W.Zuo) is very grateful to Prof. T. Gaitanos for helpful discussions. The work is supported in part by the Chinese Academy of Science Knowledge Innovation Project (KJCX2-SW-N02), the Major State Basic Research Development Program of China (G2000077400), and the Major Prophase Research Project of Fundamental Research of the Ministry of Science and Technology of China (2002CCB00200), the National Natural Science Foundation of China (10235030, 10175082) and DFG, Germany.

- 
- [1] G. Bertsch and P. J. Siemens, Phys. Lett. **B 126** (1983) 9.
  - [2] M. Schmidt, T. Hippler, J. Donges and W. Kronmüller et al., Phys. Rev. Lett. **87** (2001) 203402.
  - [3] F. Gobet, B. Farizon, M. Farizon et al., Phys. Rev. Lett. **87** (2001) 203401; Phys. Rev. Lett. **89** (2002) 183403.
  - [4] O. Lopez, Nucl. Phys. **A 685** (2001) 246.
  - [5] S. D. Gupta, A. Z. Mekjian and M. B. Tsang, Adv. Nucl. Phys. **26** (2001) 91.
  - [6] T. Matsui and F. Satz, Phys. Lett. **B 178** (1986) 416; G. F. Burgio, M. Baldo, H.-J. Schulze and P. K. Sahu, Phys. Rev. **C 66** (2002) 025802.
  - [7] P. Bonche, S. Levit and D. Vautherin, Nucl. Phys. **A 427** (1984) 278; Nucl. Phys. **A 436** (1985) 256.
  - [8] H. Müller and B. D. Serot, Phys. Rev. **C 52** (1995) 2072.
  - [9] M. Prakash, I. Bombaci, M. Prakash, P. J. Ellis, J. M. Lattimer, and R. Knorren, Phys. Rep. **280** (1997) 1; K. Strobel, C. Sohaab and M. K. Weigel, Astron. Astrophys. **350** (1999) 497; G. F. Marranghello, C. A. Z. Vasconcellos and M. Dilling, Int. J. Mod. Phys. **E 11** (2002) 83.
  - [10] R. Stock, R. Bock, R. Brockman, J. W. Harris, A. Sandoval, and H. Stroebele, Phys. Rev. Lett. **49** (1982) 1236.
  - [11] C. Fuchs, O. Essler, T. Gaitanos, H. H. Wolter, Nucl. Phys. **A 626** (1997) 987; T. Gaitanos, M. Colonna, M. Di Toro, and H. H. Wolter, arXiv:nucl-th/0403005, Phys. Lett. **B**, inpress.
  - [12] E. B. Baron, J. Cooperstein and S. Kahana, Nucl. Phys. **A 440** (1985) 744.
  - [13] H. R. Jaqaman, A. Z. Mekjian and L. Zamick, Phys. Rev. **C 27** (1983) 2782; R. K. Su, S. D. Yang and T. T. S. Kuo, Phys. Rev. **C 35** (1987) 1539.
  - [14] J. M. Lattimer, C. J. Pethick, D. G. Ravenhall, and D. Q. Lamb, Nucl. Phys. **A 432** (1985) 646; D. Catalano, G. Giansiracusa and U. Lombardo, Nucl. Phys. **A 681** (2001) 390; N. K. Glendenning, Nucl. Phys. **A 469**, (1987) 600.
  - [15] R. B. Wiringa, V. Fiks and A. Fabrocini, Phys. Rev. **C 38** (1988) 1010; A. Akmal and V. R. Pandharipande, Phys. Rev. **C 56** (1997) 2261.

- [16] I. Bombaci and U. Lombardo, Phys. Rev. **C 44** (1991) 1892.
- [17] W. Zuo, I. Bombaci, and U. Lombardo, Phys. Rev. **C 60** (1999) 024605.
- [18] D. Alonso and F. Sammarruca, arXiv:nucl-th/0301032.
- [19] C. Fuchs, Lect. Notes Phys. **641** (2004) 119, and references therein.
- [20] B. Friedman and V. R. Pandharipande, Nucl. Phys. **A 361** (1981) 502.
- [21] B. ter Haar and R. Malfliet, Phys. Rep. **149** (1987) 207.
- [22] M. Baldo, G. Giansiracusa, U. Lombardo, I. Bombaci, and L. S. Ferreira, Nucl. Phys. **A583** (1995) 599c.
- [23] H. Huber, F. Weber and M. K. Weigel, Phys. Rev. **C 57** (1998) 3484.
- [24] I. Bombaci, T. T. S. Kuo and U. Lombardo, Phys. Rep. **242** (1994) 165.
- [25] W. Zuo, A. Lejeune, U. Lombardo and J.-F. Mathiot, Nucl. Phys. **A 706** (2002) 418.
- [26] P. Grangé, A. Lejeune, M. Martzolff and J.-F. Mathiot, Phys. Rev. **C 40** (1989) 1040.
- [27] R. B. Wiringa, V. G. J. Stoks, and R. Schiavilla, Phys. Rev. **C 51**, (1995) 38.
- [28] R. Machleidt, Adv. Nucl. Phys. **16** (1989) 189.
- [29] A. Lejeune, P. Grangé, M. Martzolff and J. Cugnon, Nucl. Phys. **A 453** (1986) 189.
- [30] J. P. Jeukenne, A. Lejeune and C. Mahaux, Phys. Rep. **25c** (1976) 83.
- [31] M. Baldo, The Many-body Theory of the Nuclear Equation of State in *Nuclear Methods and the Nuclear Equation of State*, Ed. M. Baldo, (World Scientific, Singapore, 1999), Chapt.1, P.1.
- [32] M. Baldo, I. Bombaci, L. S. Ferreira, G. Giansiracusa, and U. Lombardo, Phys. Lett. **B 215** (1988) 19.
- [33] H.Q. Song, M. Baldo, G. Giansiracusa and U. Lombardo, Phys. Rev. Lett. **81** (1998) 1584.
- [34] B.D. Serot and J. D. Walecka, Adv. Nucl. Phys. **16** (1986) 1; Int. Journ. Mod. Phys. **E 6** (1997) 515.
- [35] G. E. Brown, W. Weise, G. Baym and J. Speth, Comments Nucl. Part. Phys. **17** (1987) 39.
- [36] M. Baldo, I. Bombaci and G. F. Burgio, Astron. Astrophys. **328** (1997) 274.
- [37] S. Ray, J. Shamanna and T. T. S. Kuo, Phys. Lett. **B392** (1997) 7.

FIG. 1: Diagrams of the microscopic TBF adopted for the present calculations, taken from Ref.[26]

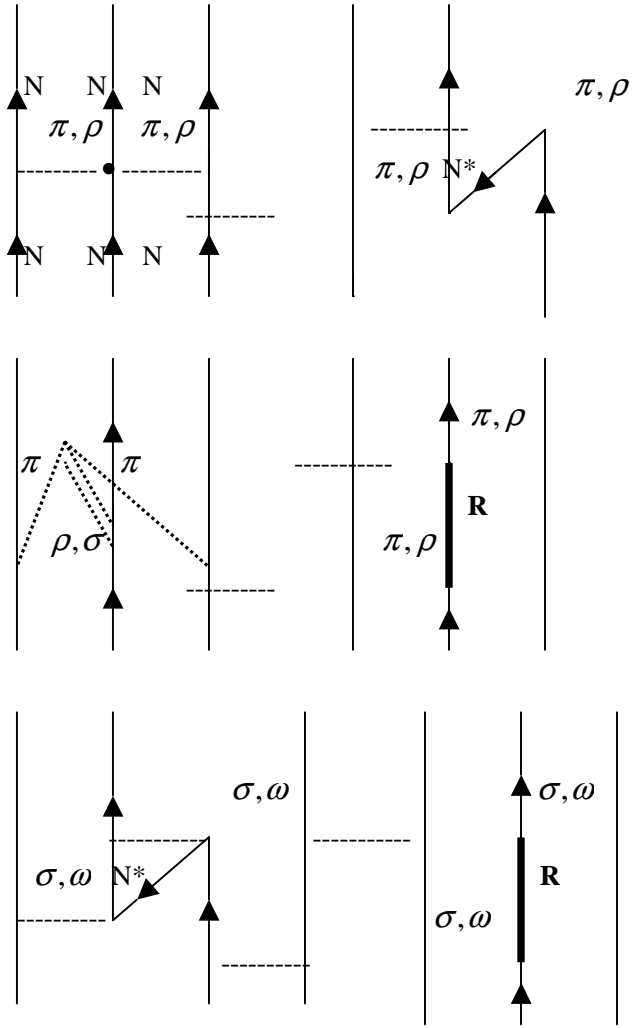
FIG. 2: Pressure as a function of density with six isotherms corresponding to  $T = 0, 8, 10, 12, 14, 16 \text{ MeV}$  from the bottom to the top for different isospin asymmetries  $\beta = 0, 0.3, 0.5$  and  $0.8$ . The solid and dashed curves represent the results with and without TBF contribution.

FIG. 3: Pressure as a function of density for symmetric nuclear matter at six values of temperature  $T = 0, 8, 10, 12, 14 \text{ MeV}$  from the bottom to the top. The dashed curves are obtained by adopting the full TBF, while the solid ones by including only the  $2\sigma - \text{NN}$  contribution of the TBF.

FIG. 4: Pressure as a function of density at a fixed temperature  $T = 5 \text{ MeV}$  for different asymmetric parameters  $\beta = 0, 0.2, 0.4, 0.6, 0.81$ . from the bottom to the top. The solid and dashed curves are the results with and without the TBF contribution, respectively.

FIG. 5: Region of mechanical instability at a fixed temperature  $T = 5 \text{ MeV}$  for both cases including the TBF (solid curve) and without the TBF (dashed curve).





**Fig.1**

